RESEARCH ARTICLE

Pectoral fin kinematics and motor patterns are shaped by fin ray mechanosensation during steady swimming in *Scarus quoyi*

Brett R. Aiello[1,*], Aaron M. Olsen[1], Chris E. Mathis[2], Mark W. Westneat[1,2] and Melina E. Hale[1,2,*]

ABSTRACT

For many fish species, rhythmic movement of the pectoral fins, or forelimbs, drives locomotion. In terrestrial vertebrates, normal limb-based rhythmic gaits require ongoing modulation with limb mechanosensors. Given the complexity of the fluid environment and dexterity of fish swimming through it, we hypothesize that mechanosensory modulation is also critical to normal fin-based swimming. Here, we examined the role of sensory feedback from the pectoral fin rays and membrane on the neuromuscular control and kinematics of pectoral fin-based locomotion. Pectoral fin kinematics and electromyograms of the six major fin muscles of the parrotfish, *Scarus quoyi*, a high-performance pectoral fin swimmer, were recorded during steady swimming before and after bilateral transection of the sensory nerves extending into the rays and surrounding membrane. Alternating activity of antagonistic muscles was observed and drove the fin in a figure-of-eight fin stroke trajectory before and after nerve transection. After bilateral transections, pectoral fin rhythmicity remained the same or increased. Differences in fin kinematics with the loss of sensory feedback also included fin kinematics with a significantly more inclined stroke plane angle, an increased angular velocity and fin beat frequency, and a transition to the body-caudal fin gait at lower speeds. After transection, muscles were active over a larger proportion of the fin stroke, with overlapping activation of antagonistic muscles rarely observed in the trials of intact fish. The increased overlap of antagonistic muscle activity might stiffen the fin system in order to enhance control and stability in the absence of sensory feedback from the fin rays. These results indicate that fin ray sensation is not necessary to generate the underlying rhythm of fin movement, but contributes to the specification of pectoral fin motor pattern and movement during rhythmic swimming.

KEY WORDS: EMG, Fish, Propulsion, Motor control, Sensory feedback, Transection

INTRODUCTION

The pectoral fins of fishes perform dual and interacting roles as motors and sensors. As motors, the pectoral fins are used during posture maintenance, maneuvering and braking (Higham et al., 2005), and serve as primary locomotor propulsors for many species (Walker and Westneat, 1997, 2002a,b). As mechanosensors, the pectoral fins respond to fin ray bending, and the sensory nerves innervating the fin rays encode fin ray movement, speed of

[1]Department of Organismal Biology and Anatomy, University of Chicago, Chicago, IL 60637, USA. [2]The College, University of Chicago, Chicago, IL 60637, USA.

*Authors for correspondence (mhale@uchicago.edu, braiello@uchicago.edu).

B.R.A., 0000-0001-9034-0460; A.M.O., 0000-0003-4398-3126; M.W.W., 0000-0002-3548-7002; M.E.H., 0000-0001-5194-1220

movement and position (Williams et al., 2013; Hardy et al., 2016; Aiello et al., 2017, 2018). In bluegill sunfish (*Lepomis macrochirus*), pectoral fin sensory feedback is necessary for generating normal hovering behavior, and the loss of feedback results in atypical kinematics, higher fin beat frequencies and reduced pectoral fin ray curvature throughout the fin stroke (Williams and Hale, 2015). Further, a behavioral analysis of bluegill sunfish navigating a complex environment found that fish use their pectoral fins to touch obstacles and, in the absence of other sensory modalities (e.g. lateral line and vision), obstacle tapping increases (Flammang and Lauder, 2013). Together, these studies indicate that pectoral fin ray sensory feedback integrates into the activity of motor control circuits to modulate motor output and swimming behaviors.

The role of mechanosensation in locomotion has also been studied in terrestrial animals. The loss of mechanosensation significantly impairs the ability to complete complex and precise movements (Cooper et al., 1993). For example, while typical limb rhythms can still be observed after the loss of sensory feedback in vertebrates (e.g. Brown and Sherrington, 1912; Sherrington, 1913), central pattern generator (CPG)-driven movement occurs with atypical kinematics (Polit and Bizzi, 1978, 1979; Bosco and Poppele, 2001), reduced accuracy and adaptability (Grillner, 1975; Sanes et al., 1985; Nathan et al., 1986), and other sensory modalities, such as vision, are required to provide compensatory feedback on limb movements (e.g. Sanes et al., 1985).

Despite the presence of atypical kinematics, only slight changes to the timing and intensity of muscle activity occur after the loss of sensory feedback (Székely et al., 1969; Hnik et al., 1982; Thoumie and Do, 1996). For example, the duration of muscle activity patterns is more variable and the consistent order of activation among a synergistic suite of muscles is not always retained after the loss of sensory feedback (Székely et al., 1969; Grillner and Zangger, 1984). Studies in tetrapods also note that the activity in some muscles increases in both intensity and duration after the loss of sensory feedback (Székely et al., 1969; Grillner and Zangger, 1975; Perret and Cabelguen, 1976, 1980). Similar results have been found in other systems. For example, after the loss of sensory feedback from the wings of insects, the activity in elevator muscles increased in intensity and became more variable (Wilson and Gettrup, 1963; Pearson and Wolf, 1987), and elevators fired later in the wing phase, overlapping with the subsequent firing of depressors (Pearson and Wolf, 1987).

In fishes, the movement and the shape of the pectoral fins are controlled through a suite of proximal muscles. Muscles attaching to the proximal portion of each fin ray allow for independent actuation and control of its movement (Westneat, 1996) and, thus, of the fin as a whole (Geerlink and Videler, 1987; Lauder et al., 2011). Fishes are suggested to be capable of actively controlling the stiffness and curvature of individual fin rays through the differential activity of their antagonistic muscles (Geerlink and Videler, 1987; Alben et al., 2007; Lauder et al., 2011). In comparison to rigid structures, an

advantageous deformation pattern of a flexible propulsor (e.g. insect wings and the fins of fishes) can increase propulsive capability (Daniel and Combes, 2002), locomotor efficiency (Yamamoto et al., 1995; Zhu and Shoele, 2008; Young et al., 2009) and maneuverability (Tangorra et al., 2010; Lauder et al., 2011; Flammang et al., 2013).

Here, we examined how the loss of fin ray mechanosensation impacts pectoral fin muscle activity patterns and kinematics during labriform (pectoral fin-based) swimming. This is the first study to examine the effect of fin ray denervation on propulsive swimming and the first to assess the impact of denervation on muscle activity during any rhythmic fin movement. We hypothesized that pectoral fin ray proprioceptive feedback helps regulate the activity patterns of muscles actuating the fin, and the loss of fin ray proprioception will lead to increased variance in fin kinematics and muscle activity. To test these hypotheses, electromyograms of the six major fin muscles and synchronized 3D kinematics were recorded from the pectoral fin of the parrotfish, *Scarus quoyi*. Next, we performed bilateral transection of all sensory nerves innervating the pectoral fin rays, and examined the effects on 3D fin kinematics and the activity patterns of the muscles that actuate the fin. In this study, we focused on loss of sensory input from the fin rays and membrane and did not disrupt more proximal innervation of the fin.

MATERIALS AND METHODS
Fish specimens and experimental overview
Six terminal phase male parrotfish, *Scarus quoyi* Valenciennes 1840, were used in this study (standard length range 11.5–15.5 cm, mean±s.d. 13.15±1.67 cm). Parrotfish were obtained commercially and housed in aquaria equipped with recirculating water filters. Water temperature was maintained at ~23°C and the fish were exposed to a 12 h:12 h light:dark cycle. Before each experiment, each fish was anesthetized in a solution of MS-222 (0.25 g l^{-1}). Bilateral incisions were made through the skin and the connective tissue overlaying the medial side of the most proximal portion of the left and right pectoral fins to expose the sensory nerves innervating the pectoral fin rays. In previous work, no difference in bluegill sunfish pectoral fin hovering kinematics was found before and after the conduction of sham experiments, where a skin incision was made to expose the intact pectoral fin ray nerves (Williams and Hale, 2015). Further, in this study, the performance of surgery prior to control swimming ensured that differences in kinematics and motor patterns between trials before and after the loss of sensory feedback (nerve transection) were due to the loss of sensory feedback and not to the effects of surgery. A single bipolar electrode was then inserted into each of the six major muscles actuating the left pectoral fin. Fish were allowed to recover, placed in a flow tank, and then swam at a speed of 2 body lengths (equivalent to total length) per second (BL s^{-1}). After each fish completed its control swimming trials, it was lightly anesthetized and the already exposed sensory nerves were transected. The sensory nerves were initially identified in prior work using immunohistochemistry (Thorsen and Hale, 2007; Williams et al., 2013), and confirmed through dissection in *S. quoyi* prior to experimentation. The nerves are completely superficial to the underlying musculature and only innervate the fin rays and membrane of the fin. The fish was allowed to recover and was then placed back in the flow tank to repeat the swimming procedure. 3D kinematics and motor control patterns were recorded and analyzed at 2 BL s^{-1} before and after the loss of fin ray sensory feedback. Finally, the speed at which each fish transitioned from the pectoral fin to body-caudal fin (BCF) gait was measured before and after afferent nerve transection. Flow speed was increased in a step-wise manner where speed was increased by 0.5 BL s^{-1}, stabilized for

1 min, then increased again by 0.5 BL s^{-1}. Flow speed was increased in this manner until the fish transitioned to the BCF gait. All experimental procedures were carried out under University of Chicago Institutional Animal Care and Use Committee guidelines (protocol 72365 to M.W.W.; protocol 71589 to M.E.H.).

Surgical procedures and electrode implantation
Surgery and electromyography (EMG) electrode implantation followed published methods (Westneat and Walker, 1997; Aiello et al., 2014). Electrodes were made using 0.005 mm diameter insulated stainless steel bipolar wire (California Fine Wire, Grover Beach, CA, USA). After approximately 0.5 mm of insulation was stripped from the tip of each monopole, the wire was fed through a 26 gauge needle and formed into a twist hook (Loeb and Gans, 1986). A single electrode was placed in six different muscles: three lateral muscles [arrector ventralis (ARV), abductor profundus (ABP), abductor superficialis (ABS)] and three medial muscles [arrector dorsalis (ARD), adductor profundus (ADP), adductor superficialis (ADS)] (Fig. 1). Hot glue was then used to bind the six wires together into a single cable, which was subsequently run dorsally and sutured to the base of the first ray of the dorsal fin. These six electrodes were left in throughout the duration of the experiment and were the same electrodes used for EMG recordings after nerve transection. Upon completion of the experiment, animals were killed in a high concentration of MS-222 and electrode implantation was confirmed post mortem.

Data acquisition
EMG and kinematic recordings took place after the fish had recovered for approximately 1–2 h after surgery. EMG signals were amplified by a factor of 10,000, bandpass filtered from 30 Hz to 6 kHz, and notch filtered at 60 Hz using a Grass amplifier (Model 15LT, Grass Technologies, Astro-MED Inc., West Warwick, RI, USA). Signals were then acquired and saved to a computer at 5000 Hz using PolyVIEW16 software (Grass Technologies) after being passed through a Grass PVA-16 A/D converter (Grass Technologies).

EMG recordings were collected while each fish was filmed swimming in a flow tank (Vogel and Labarbera, 1978) with a total volume of 360 l and working volume dimensions of 30 cm×30 cm×60 cm. Fish were filmed at 500 frames s^{-1} with three synchronized Photron high-speed digital video cameras at 1024×1024 pixel spatial resolution (FASTCAM APX-RS, FASTCAM SA7 and Mini UX 100, Photron, San Diego, CA, USA). Two cameras with lateral views were placed with slightly offset angles and the third camera was placed at an equal distance from the tank and filmed the ventral view of the fish using a mirror placed below the flow tank working area at an angle of 45 deg. EMG and video data were synchronized with the application of a time stamp on the EMG record.

EMG and kinematic analysis
For each trial, video and EMG data were analyzed for five continuous fin stroke cycles. Basic kinematic data (abduction onset and duration, adduction onset and duration, and the lag time between consecutive fin strokes) were collected for each fin stroke. In our four-phase fin stroke, the protraction period began after the fin ceased adduction and began to protract forward, the abduction period began as soon as the fin began to abduct more than 1 deg from its position at the termination of adduction, fin reversal occurred during the short duration after the fin ceased abducting and before it began adducting, and adduction began as soon as the fin adducted more than 1 deg from its fully abducted position. EMG
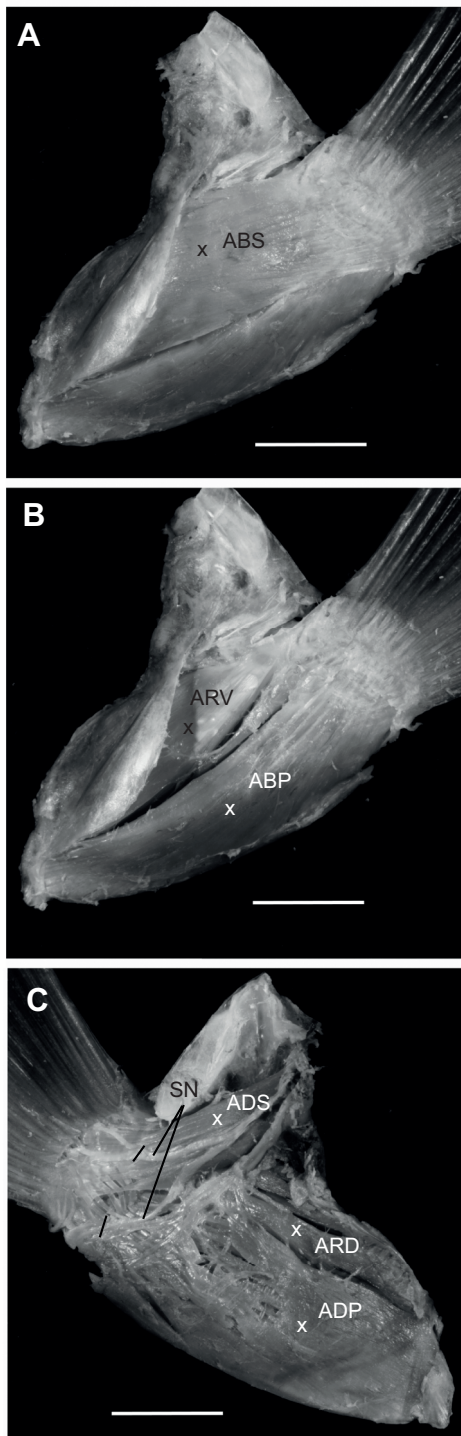
Fig. 1. Pectoral muscles of *Scarus quoyi*. (A) Lateral view of the abductor superficialis (ABS) muscle overlying the abductor profundus (ABP). (B) Lateral view with ADS removed, revealing the arrector ventralis (ARV) and ABP. (C) Medial view of same fin, with the brachial plexus nerves visible, including the sensory nerves (SN) entering the fin blade, with the point of transection for deafferentation (black lines) and electrode placement in the ADS, ARD and ADP muscles indicated. Crosses show electrode placement. Scale bars: 1 cm. Field Museum of Natural History specimen ID number: FMNH 110860.

data were analyzed using a custom MATLAB (MathWorks, Natick, MA, USA) routine (Jose Iriarte-Diaz, University of Illinois-Chicago). For each EMG burst, the onset time (EMG_{on}), offset

time (EMG_{off}), duration ($EMG_{dur}=EMG_{off}-EMG_{on}$), time of peak amplitude (EMG_{peak}) and rectified integrated area (RIA) were calculated. Variables were calculated in absolute time (seconds) and converted to a percentage of the fin stroke cycle relative to the start of pectoral fin abduction.

In a subset of the individuals ($N=4$; standard length range 12.2–15.5 cm, mean±s.d. 13.80±1.69 cm), 3D pectoral fin kinematics were also collected. Videos were digitized using the StereoMorph package (Olsen and Westneat, 2015) in R (http://www.R-project.org/). In at least two views for every other video frame, the tip and base of the leading edge fin ray were digitized as landmarks and a curve (described by 50 evenly spaced points or semi-landmarks) was fitted along the length of the ray. The tip and base of the trailing edge fin ray and most central fin ray were also digitized. Several body landmarks were also digitized in at least two views for every 10 video frames: the rostral tip of the dorsal beak, the left eye, the base of the left and right pelvic fins, the most rostral attachment of the anal fin, the most rostral intersection of the left and right opercula, and several midline natural skin coloration markings that were unique to each fish. Several variables were then calculated over the length of each fin stroke: the fin angle relative to the fully adducted position (stroke amplitude), leading edge fin ray curvature, the 3D path of the leading edge fin ray tip, angular velocity and acceleration, and stroke plane angle relative to the anterior–posterior (AP), dorsal–ventral (DV) and medial–lateral (ML) axes. The 2D stroke plane angle (β) was calculated following the methods of Walker and Westneat (1997). To measure 3D stroke plane angle, we first fitted a plane, using the 'svd' function in R (http://www.R-project.org/), to body-aligned leading edge base and tip landmarks superimposed over a complete stroke (downstroke and upstroke). In this way, the plane describes the orientation of the space traversed by the leading fin ray during a complete stroke relative to the body. This plane is also oriented approximately orthogonal to the surface of the pectoral fin. We then projected the three body axes into the stroke plane to create projected body axis vectors, parallel to the stroke plane but also parallel to a corresponding body plane. The craniocaudal (AP) axis (X) was projected so that it was parallel to the sagittal plane, the DV axis (Y) was projected so that it was parallel to the coronal plane, and the ML axis (Z) was projected so that it was parallel to the transverse plane. Each stroke plane angle (AP, DV and ML) was then calculated as the angle between each body axis and the corresponding projected body axis vector (see Fig. S2A). Pectoral fin chord-wise camber was also calculated by fitting a plane to the four corners of the fin (leading edge base, leading edge tip, trailing edge base, trailing edge tip) and then calculating the distance between this plane and the tip of the central fin ray. Larger distances are indicative of larger degrees of chordwise bending (camber). To test whether tip trajectories differed significantly between test and transection strokes, we used shape analysis, treating the trajectory of the leading edge fin ray tip (defined by the 3D coordinate at 75 proportional time points) for each fin stroke ($N=41$; 19 control and 22 transection) as a separate shape. We used Procrustes superimposition to optimally align the tip trajectories for each stroke with each other and principal components analysis (PCA) to identify the major axes of variation in trajectory shape. We then used t-tests to test for significant differences in mean trajectory shape along each of the first three PC axes. Excluding rotation of the trajectory shapes in the Procrustes alignment did not change the conclusions.

Statistical analyses were performed on the data in R 3.2.1 (http://www.R-project.org/) and JMP 9.0.1 (SAS, Cary, NC, USA). The rhythmicity of the fin stroke cycle (relative variance in the cycle period) was calculated as the coefficient of variation (Ross et al.,

2013): CV=(s.d./mean)×100 (Sokal and Braumann, 1980). The CV was also calculated for fin beat frequency, EMG_{on}, EMG_{dur}, EMG_{peak} and RIA before and after the loss of sensory feedback (transection) as a standardized measure of variation in the data. Student's t-tests were also used to test for significant differences between the control and transection trials for several variables: fin beat frequency, EMG_{on}, EMG_{dur}, EMG_{peak}, RIA and the CV of each of these variables. A PCA of the 3D shape of the fin stroke trajectory was conducted in R following published methods (Olsen, 2017), and each fin stroke was treated as a unique species. Finally, the lm (linear model) and aov (analysis of variance) functions were used to conduct a multi-factor ANOVA in R to test for significant differences in 3D kinematic variables before and after the loss of

sensory feedback. The factors in the ANOVA were individual and experimental group (control or transection), and all P-values were adjusted for multiple comparisons.

RESULTS

Pectoral fin kinematics before and after loss of sensory function

The pectoral fin beat cycle can be divided into four main phases: a protraction period where the fin is protracted before the start of abduction, abduction (downstroke), a short reversal period where the fin is rotated about its long axis to reorient the leading edge between abduction and adduction, and adduction (upstroke) (Fig. 2).
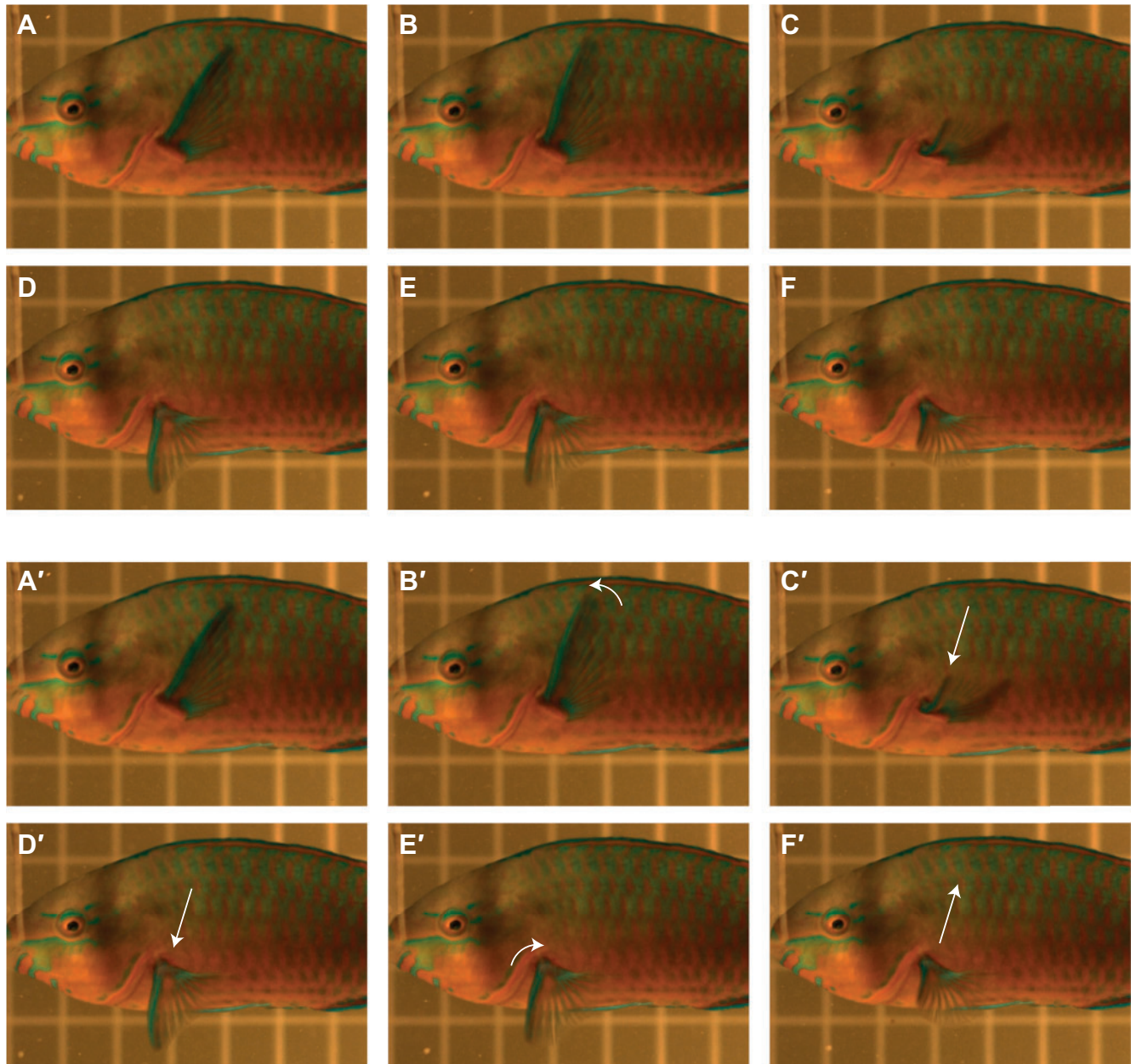
Fig. 2. Summary images of pectoral fin stroke components. (A,B) The pectoral fin cycle begins with a protraction period where the fin is held against the body wall and protracted before the start of abduction. (B–D) Next, downstroke begins and the fin is abducted. (D,E) A short reversal period occurs between abduction and adduction where the fin is rotated about its long axis to reorient the leading edge. (E,F) The final component of the fin stroke is upstroke, where the fin undergoes adduction. Edited image sequences (A′–F′) are shown below the corresponding original image sequences (A–F). The white arrows illustrate the trajectory taken between the previous frame and the current frame for a given panel.

Table 1. Summary kinematics before (control) and after transection

	% Protraction	% Abduction	% Reversal	% Adduction	Frequency (Hz)	Duration (s)	Duration CV	N
Before	8.20±3.34	42.33±4.19	4.35±4.32	45.12±4.61	4.78±1.02	0.22±0.05	9.71±7.33	6
	P=0.001	P=0.769	P=0.081	P=0.001	P=0.0002	P=0.0001	P=0.754	
After	5.40±3.27	42.62±3.81	2.96±1.42	49.01±4.38	5.71±0.87	0.18±0.03	8.57±4.55	6

Data are means±s.d. for trials before and after transection. Swimming speed is was 2 BL s^{-1}.
All P-values have been adjusted for multiple comparisons.

Fin beat frequency, fin beat rhythmicity, and the speed at which each fish transitioned from the pectoral to BCF gait were measured before and after the loss of fin ray sensory feedback. In fish with an intact sensory pectoral fin ray sensory system, fin beat frequency averaged 4.78±1.02 Hz and significantly increased to 5.71±0.87 Hz (Table 1, Fig. 3A) after nerve transection. Fin beat rhythmicity was measured by calculating the CV of fin beat duration (Table 1). In intact fish, fin beat duration CV averaged 9.71±7.33. After the loss of fin ray sensory feedback, the CV of fin beat duration was not significantly different and averaged 8.57±4.55. The speed at which the transition between the pectoral fin and BCF gait occurred significantly decreased from 4.80±0.57 BL s^{-1} prior to transection to 3.40±0.55 BL s^{-1} after transection (Fig. 3B, Table 2).

The loss of sensory feedback impacted the relative proportion occupied by each component of the fin cycle (Table 1). The loss of sensory feedback resulted in a shorter protraction phase (P=0.001) and longer adduction phase (P=0.001). The portion of the fin cycle dedicated to abduction and reversal did not change after the loss of fin ray sensory feedback (P>0.05). However, after the loss of sensory feedback, the absolute duration of each fin stroke phase was significantly shorter (P<0.05). The protraction, abduction, reversal and adduction phases decreased from 0.018±0.01 to 0.009±0.0057 s, 0.092±0.021 to 0.0764±0.014 s, 0.009±0.008 to 0.005±0.002 s, and 0.099±0.025 to 0.088±0.017 s, respectively, before and after the loss of fin ray sensory feedback.

3D analysis of the fin stroke before and after loss of sensory feedback

We conducted an analysis of 3D pectoral fin kinematics to analyze the impact of the loss of fin ray sensory feedback on the subtler parameters of a fin stroke that could impact hydrodynamic performance. A 3D outline of the trajectory of the leading edge fin ray tip throughout the fin stroke revealed a figure-of-eight pattern when viewed laterally (Fig. 4A). In intact individuals, the fin beat amplitude, measured as the angle between the body and the leading edge fin ray, averaged 65.88±10.86 deg at peak downstroke (Fig. 5, Table 3). The fin AP, DV and ML 3D stroke plane angles averaged 54.40±10.18, 62.02±19.97 and 20.41±12.57 deg, respectively (Table 3; Fig. S2A). Maximum angular velocity calculated using 3D kinematics was similar during the downstroke and upstroke and occurred at 23.08±2.93% and 70.30±5.00% fin cycle, respectively (Fig. 5C, Table 3). Maximum angular acceleration always occurred near mid-stroke (Fig. 5D, Table 3). Finally, peak leading edge fin ray curvature occurred just before the fin reached maximum velocity during the downstroke and just after the fin reached maximum velocity during the upstroke. Peak curvature averaged 0.027±0.005 mm^{-1} during the downstroke and 0.020±0.005 mm^{-1} during the upstroke (Fig. 5, Table 3). The maximum chordwise camber of the fin averaged 5.66±1.02 mm during the downstroke and 5.40±1.63 mm during the upstroke (Table 3).

3D pectoral fin kinematics at 2 BLs^{-1} were also measured after the loss of sensory feedback. The average duration of the protraction period was shorter after transection. The fin stroke was significantly altered after the loss of sensory feedback. The AP stroke plane angle was significantly greater after the loss of sensory feedback (adjusted P<0.0001; Figs S1 and S2, Table S1; Table 3), increasing by approximately 10 deg to an average of 65.36±6.68 deg (Table 3; Fig. S2A) after transection. Finally, the angular velocity of the downstroke was significantly greater after the loss of sensory feedback (adjusted P=0.027; Fig. S1, Table S1).

Several 3D kinematic variables were not significantly different after the loss of sensory feedback (Fig. S1, Table S1; Table 3). A PCA showed that the trajectory of the fin stroke was not significantly different after the loss of sensory feedback when differences in stroke plane angle were taken into account (Fig. S2B). For the PC1 comparison, P=0.07 when corrected for differences in stroke plane and P=0.04 when differences in stroke plane are not taken into account; all comparisons for PC2 and PC3 resulted in P>0.05. The amplitude of the fin stroke, peak leading edge fin ray curvature during the downstroke and upstroke, the time at which each curvature peak occurred within the fin cycle, and the average maximum chordwise camber during the upstroke and downstroke were not significantly different after the loss of sensory feedback (adjusted P>0.05; Fig. S1, Table S1; Fig. 5, Table 3). Using the 3D kinematics we also found that the maximum angular acceleration,
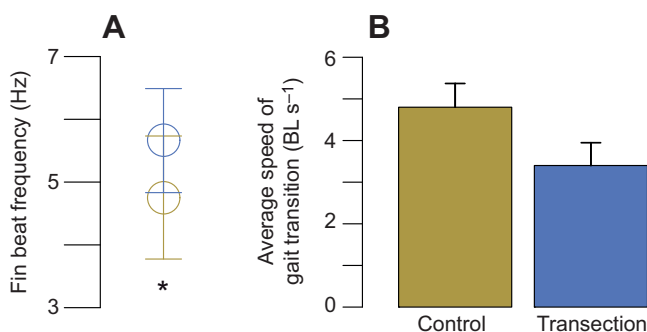

Fig. 3. Pectoral fin kinematics before and after the loss of sensory feedback. (A) Fin beat frequency is significantly greater after the loss of sensory feedback (blue) in comparison to control trials (green). (B) In control trials, the transition between the pectoral fin and the body-caudal fin (BCF) gait occurs at a significantly slower speed after the loss of sensory feedback [between 4 and 5 body lengths (BL) s^{-1}].

**Table 2. Speed of gait transition before and after the loss of fin ray sensory feedback**

Individual	Before	After
2	5.5	4
3	4.5	3
4	5	4
5	5	3
6	4	3
Means±s.d.	4.8±0.57	3.4±0.55
	P=0.00417822	

Speed is given in units of BL s^{-1}.
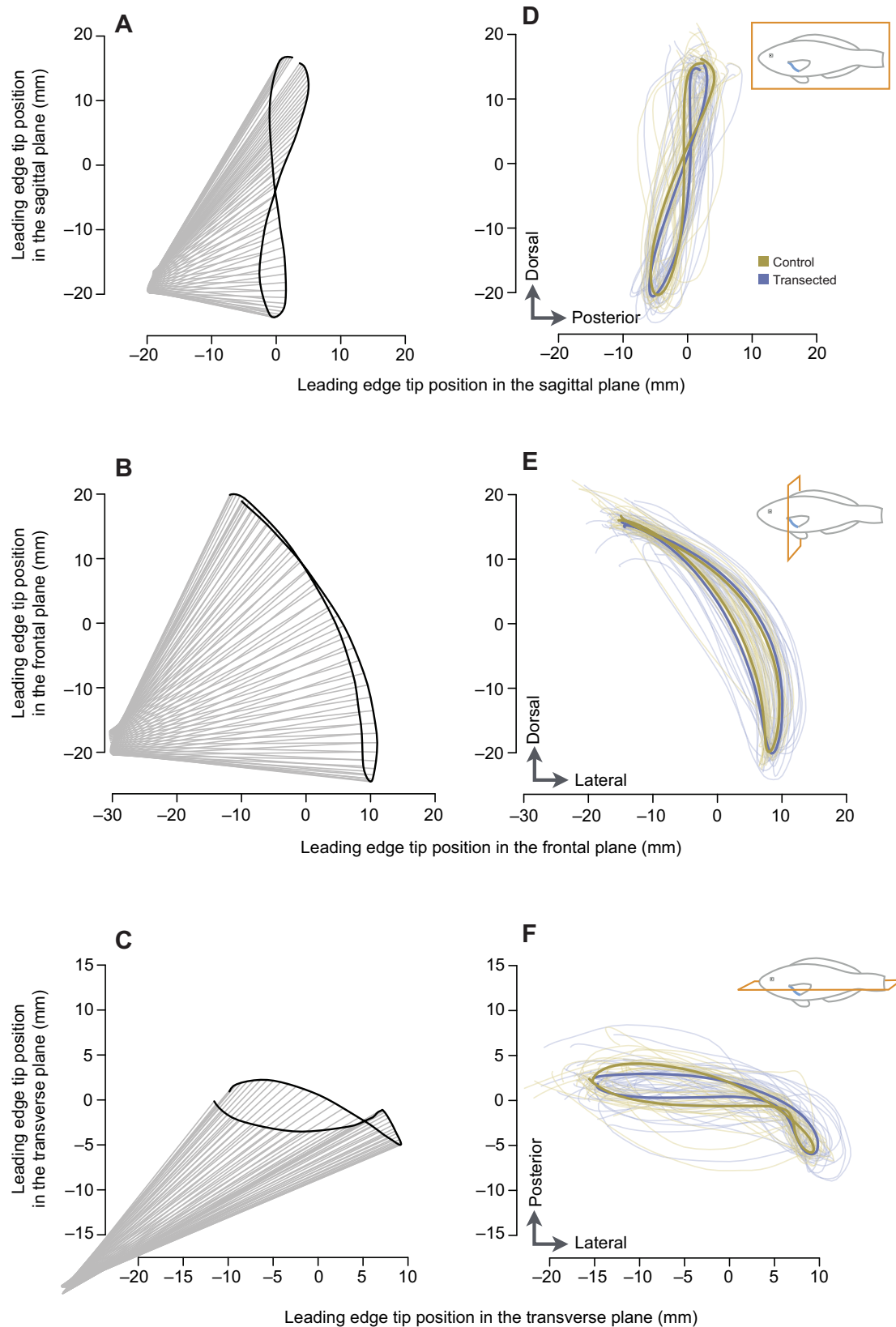
Fig. 4. Trajectory of the leading edge pectoral fin ray at 2 BL s⁻¹. The tip of the leading edge fin ray was traced in trials before and after the loss of sensory feedback. The trajectory of the fin stroke is shown projected in the sagittal (A,D), frontal (B,E) and transverse (C,F) planes (see insets) for a single fin stroke (A–C) and summarized across all individuals (D–F) before and after the loss of sensory feedback. This representation of the fin stroke trajectory removes the effects of fin stroke plane angle (the orientation of the fin stroke relative to the body in each plane). After the differences in fin stroke angle were removed, there were no significant differences between trials before and after the loss of sensory feedback (see Fig. S3 for fin stroke shape principal components analysis). Bold lines in D–F represent group averages.
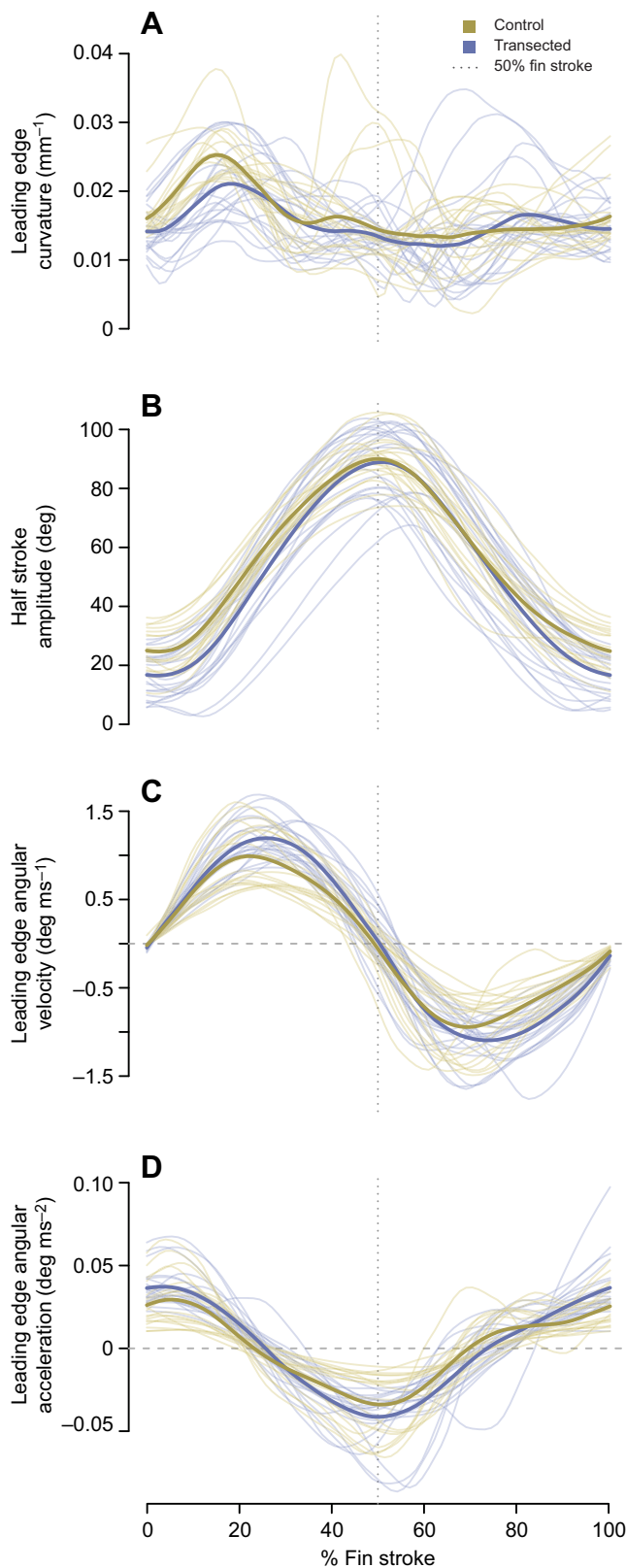
Fig. 5. Leading edge pectoral fin ray kinematics at 2 BL s⁻¹. Leading edge fin ray curvature (A), fin stroke amplitude (B), angular velocity (C) and angular acceleration (D) were measured before and after the loss of sensory feedback. For most variables, no significant differences are found between trials conducted before and after the loss of sensory feedback (Table 3). However, maximum angular velocity achieved during the downstroke was significantly greater after the loss of sensory feedback.

maximum angular velocity during the upstroke, and the proportion of the fin cycle at which maximum angular velocity was reached during the upstroke were not significantly different after transection ($P>0.05$; Fig. S1, Table S1; Fig. 5, Table 3). The 3D ML stroke plane angle also did not significantly differ after the loss of sensory feedback (mean±s.d. 16.50±11.28 deg; adjusted $P=0.598$).

Muscle activity patterns during pectoral fin swimming before and after the loss of sensory feedback

Muscle activity onset, duration and time of peak amplitude were calculated for six muscles that actuate the pectoral fin. In intact fish, activity in the three muscles of the abductor complex – ARV, ABP and ABS – began at similar times (no greater than 9.54% fin cycle between the onset of any muscles in this group), but were always activated in sequence, with a consistent order of ARV, ABP and then ABS onset (Fig. 6A; Table S2). Abductor muscle activity began before or during the fin protraction period when the fin was undergoing protraction. Similar trends were found for the adductor muscle complex of intact fish (Fig. 6A; Table S2). The three adductors were consistently activated in the following order: ARD, ADP and ADS (Fig. 6A).

The overlap in activity between antagonistic muscle pairs (ARV–ARD, ABP–ADP and ABS–ADS) was calculated across two sections of the fin stroke: (1) the span of the fin stroke that includes fin reversal, the end of abduction and the start of adduction, and (2) between consecutive fin strokes during the protraction period. Points of fin reversal and the transition between consecutive fin strokes are relevant markers within the stroke because these are the times during the fin stroke that antagonistic muscle activity is most likely to overlap. In intact fish, for each pair, there was no overlap in activity between antagonistic muscles (Fig. 7; Table S2). The overlap in activity between antagonistic muscles at the transition between consecutive fin beats (protraction period) showed similar trends to those seen at the midpoint (fin reversal between downstroke and upstroke) of each fin beat, but was lower in magnitude.

Muscle activity patterns were also recorded after pectoral fin afferents were transected (Fig. 6B; Table S2). Relative to the beginning of the fin stroke, the loss of sensory feedback resulted in significantly earlier average activity onset, later average offset, and thus an overall significant increase in activity duration for both groups of muscles ($P<0.05$; Fig. 6; Table S2). However, the relative time of peak EMG amplitude within the fin stroke did not change for any muscle after transection (Fig. S3A, Table S2). Further, muscle onset variability (CV) was not significantly different after transection ($P>0.05$; Table S2). After transection, the RIA of the EMG for each muscle was approximately double the RIA recorded in trials with an intact sensory system, and these differences were significant for each muscle ($P<0.01$; Fig. S3B, Table S2). The overlap in activity between antagonistic muscles occurring midway between the downstroke and upstroke (fin reversal period) also significantly increased for all three antagonistic pairs after transection ($P<0.0001$; Fig. 7; Table S3). Prior to transection, no overlap occurred, whereas post-transection the overlap between antagonists averaged 8.24±15.18, 9.61±18.26 and 17.38±15.31% fin cycle for the arrector, profundus and superficialis pairs, respectively. Overlap in activity between antagonistic muscles also occurred between subsequent fin strokes during the protraction period after transection and showed similar trends to the overlap occurring between the downstroke and upstroke (Table S3). After the loss of sensory feedback, overlap in activity between antagonistic muscles significantly increased during the protraction period ($P<0.0001$; Table S3).

Table 3. Summary of 3D kinematics

	Amplitude (deg)	Downstroke max. velocity deg ms⁻¹	Downstroke max. velocity % Fin cycle	Upstroke max. velocity deg ms⁻¹	Upstroke max. velocity % Fin cycle	Max. acceleration (deg ms⁻²)	Downstroke max. fin ray curvature mm⁻¹	Downstroke max. fin ray curvature % Fin cycle	Upstroke max. fin ray curvature mm⁻¹	Upstroke max. fin ray curvature % Fin cycle	Stroke plane angle (deg) β	Stroke plane angle (deg) AP	Stroke plane angle (deg) DV	Stroke plane angle (deg) ML	Max. camber (mm) Downstroke	Max. camber (mm) Upstroke
Before	65.88±10.86	1.01±0.35	23.08±2.93	−1.012±0.356	70.30±5.00	−0.034±0.019	0.027±0.005	19.05±9.88	0.020±0.005	76.53±16.65	25.44±12.39	54.40±10.18	62.03±19.97	20.41±12.57	5.66±1.02	5.40±1.63
	$P=0.0099$	$P=0.0012$	$P=0.0062$	$P=0.0058$	$P=0.2491$	$P=0.0177$	$P=0.003$	$P=0.2390$	$P=0.578$	$P=0.2325$	$P=0.047$	$\mathbf{P=4.56\times10^{-9}}$	$P=0.83$	$P=0.079$	$P=0.062$	$P=0.006$
	$P_{adj}=0.118$	$\mathbf{P_{adj}=0.022}$	$P_{adj}=0.082$	$P_{adj}=0.082$	$P_{adj}=1.00$	$P_{adj}=0.177$	$P_{adj}=0.049$	$P_{adj}=1.00$	$P_{adj}=1.00$	$P_{adj}=1.00$	$P_{adj}=0.469$	$\mathbf{P_{adj}=1.37\times10^{-7}}$	$P_{adj}=1.00$	$P_{adj}=0.598$	$P_{adj}=0.611$	$P_{adj}=0.116$
After	73.77±8.41	1.24±0.23	26.04±3.45	−1.196±0.260	72.42±5.73	−0.043±0.017	0.022±0.005	22.61±9.12	0.019±0.006	81.39±13.46	21.24±4.50	65.36±6.68	60.52±16.72	16.50±11.28	6.00±1.29	6.44±1.55

Data are means±s.d. for trials before and after transection. Swimming speed is 2 BLs⁻¹. P_{adj} are P-values adjusted for multiple comparisons; bold indicates significant differences between groups. AP, anterior–posterior plane; DV, dorsal–ventral plane; ML, medial–lateral plane. β is 2D stroke plane angle. Camber is chordwise fin camber.

DISCUSSION

In our experiments, sensory nerves that exclusively innervate the pectoral fin rays (and no associated proximal musculature) were transected between the control and experimental trials. It is likely that sensation of more proximal regions of the fin also informs movement, but it is unlikely that the muscles of teleost fishes are innervated by muscle spindles. Other than a single study in jaw muscle (Maeda et al., 1983) that has not been duplicated, spindles have not been identified in the muscles of teleost fishes despite investigation (Barker, 1974). Putative sensors have been indicated to be present in the tendons attached to the base of teleost fin rays (Pansini, 1888; Fessard and Sand, 1937; Ono, 1979), in the connective tissue associated with myotomal muscles in fishes (Ono, 1982), and in the joints and muscles associated with fins in chondrichthyans (Wunderer, 1908; Fessard and Sand, 1937; Lowenstein, 1956). While sensors innervating the proximal muscles, tendons and/or joints of the pectoral fin system have not been identified in any wrasse species, it is likely they exist and continued to provide sensory feedback during our transection experiments. Any changes in kinematics or muscle activity patterns after sensory nerve transection were entirely due to the loss of sensory feedback exclusively from the pectoral fin rays.

The effect of losing pectoral fin ray sensory feedback on pectoral fin kinematics

Pectoral fin rhythmicity is not dependent on fin ray sensory feedback: with the loss of pectoral fin ray sensory feedback in *S. quoyi*, rhythmicity was maintained or increased (Fig. 3B). It is presumed that rhythmic and coordinated pectoral fin movement is driven by a local CPG, as is the case for other vertebrate limb systems (e.g. Grillner, 1975; Grillner and Zangger, 1979; Grillner and Zangger, 1984; Grillner, 1985). For example, in tetrapods, mechanosensation provides feedback to modulate rhythmicity (Katz and Harris-Warrick, 1990) and can reinforce rhythmicity (Fuchs et al., 2012) in central pattern generating circuits. In the pectoral fin system, the maintenance of pectoral fin rhythmicity is not dependent on mechanosensory feedback from the pectoral fin rays.

We found that the pectoral fin stroke plane was significantly different after the loss of sensory feedback in *S. quoyi*. The loss of fin ray sensory feedback resulted in fin movement with a significantly greater angular velocity during the downstroke (Table 3; Figs S1, S2A), and a more vertical stroke plane caused by a significant increase in the AP stroke plane angle (Table 3; Figs S1, S2A). However, the trajectory of the fin stroke was not significantly different after the loss of sensory feedback when differences in the stroke plane angle were taken into account (Fig. 4; Fig. S3). In other words, the shape of the fin stroke was not changed after the loss of fin ray sensory feedback; however, the position of the fin throughout the fin stroke relative to the body was significantly different after the loss of fin ray sensory feedback (Table 3; Figs S1, S2A). The loss of limb sensory feedback in tetrapods often results in atypical kinematics of varying degree (Polit and Bizzi, 1978, 1979; Nathan et al., 1986; Sainburg et al., 1995). Limb movements in human patients with large-fiber sensory neuropathy are conducted with directional errors and increased velocity (Bosco and Poppele, 2001), and vision is needed to provide compensatory feedback on limb movements to reduce these effects (Sainburg et al., 1993). In most fishes, the eyes are not well positioned to view the entirety of pectoral fin movement. Therefore, our data suggest that fin ray sensory feedback is needed to properly orient and position the fin in space relative to the body.

The increase in fin beat frequency after the loss of sensory feedback could be an effect of hydrodynamic changes of the fin
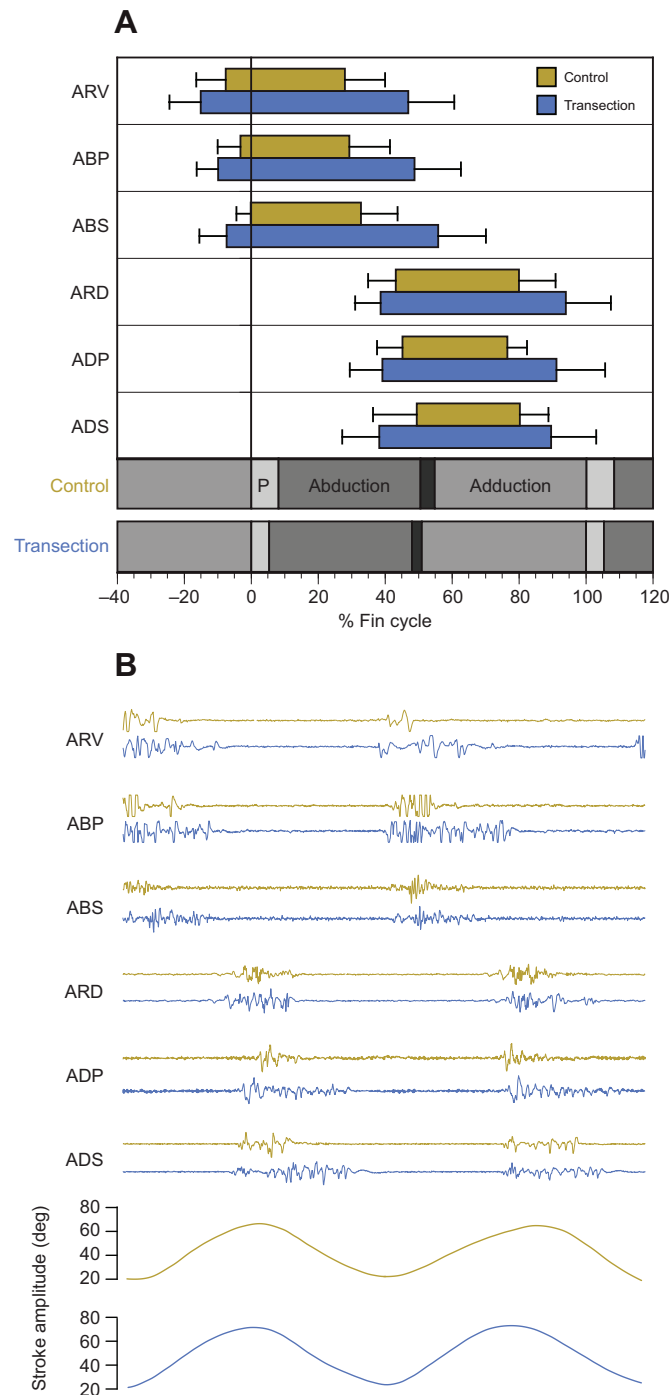
Fig. 6. Pectoral fin motor patterns before and after the loss of sensory feedback. (A) After the loss of sensory feedback, the onset of activity was earlier and the duration was prolonged in comparison with activity patterns in trials before transection at the same speed. P, protraction. (B) Raw kinematics and muscle activity patterns for two consecutive fin strokes before and after the loss of sensory feedback.

stroke. The force production of a fin stroke depends on the flow speed, angular velocity of the fin, angle of attack of the fin, the fin stroke plane angle and fin shape. The spatio-temporal patterns of fin deformation throughout the fin stroke are also known to significantly impact force production (e.g. Lauder and Drucker, 2004; Esposito et al., 2012; Flammang et al., 2013). One measure of fin deformation that significantly impacts the hydrodynamic performance of a flexible propulsion is camber. Our results indicate that there is no difference in the average maximum fin camber during the upstroke or downstroke before and after the loss of fin ray sensory feedback. All

other variables being equal, the more vertically oriented stroke plane that was used by the fish after the loss of sensory feedback could orient the lift vector more vertically and the drag vector more horizontally. As lift is often the more dominant force in flapping propulsion, a change in stroke plane angle likely results in decreased thrust per fin stroke. An increase in fin beat frequency results in increased force production per stroke (Kahn et al., 2012). *Scarus quoyi* could therefore be increasing fin beat frequency after the loss of fin ray sensory feedback as a mechanism to increase thrust production (Walker and Westneat, 1997).
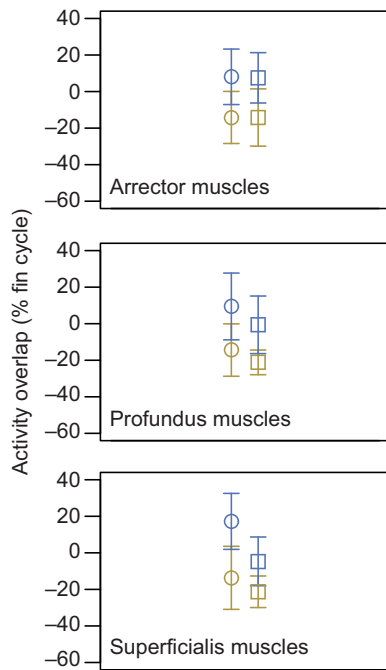
Fig. 7. The relative overlap in activity between pairs of antagonistic muscles before and after the loss of sensory feedback. Overlap in activity between antagonistic muscles was negative at a speed of 2 BL s^{-1} for the arrector and profundus pairs around the time of peak abduction (circles). A similar trend was observed across the period of peak adduction (squares). After the loss of sensory feedback, activity overlap between antagonistic muscles increased significantly. Circles represent overlap spanning the period of peak abduction, and squares represent overlap spanning the period of peak adduction.

The transition from the pectoral fin to the BCF gait occurred at a significantly slower average speed after the loss of fin ray sensory feedback in *S. quoyi* (Fig. 3, Table 2). From work on humans (Margaria, 1938), horses (Hoyt and Taylor, 1987) and fishes (Korsmeyer et al., 2002), it was also suggested that gait changes occur in order to minimize energy consumption with changing speed. In *S. quoyi* there is likely an increased energy requirement to support the increased fin beat frequency after deafferentation. If gait changes in fish are related to energy consumption, then our data fit this hypothesis. Previous work in juvenile wrasse indicates that mechanical limits can also act to trigger gait transitions in swimming fishes (Hale et al., 2006). In this study, deafferentation of pectoral fin ray nerves resulted in increased pectoral fin beat frequency, which averaged nearly 6 Hz at 2 BL s^{-1}. It is possible that frequencies of this range are reaching the biomechanical or physiological limit for a fish of this size and species, and a gait transition is necessary in order for *S. quoyi* to match high flow speeds.

The effect of losing pectoral fin ray sensory feedback on muscle activity patterns
Pectoral fin ray mechanosensation represents a significant source of sensory feedback for the adjustment of pectoral fin muscle activity patterns in *S. quoyi*. The loss of fin ray sensory feedback results in similar or more drastic changes to the activity patterns of muscles controlling locomotion compared with the loss of complete limb sensory feedback in other systems. Consistent with other systems (Grillner and Zangger, 1975; Hnik et al., 1982; Thoumie and Do, 1996), the order of activation of muscles relative to one another was unchanged after deafferentation in this study (Fig. 6B).

The maintenance of a consistent muscle activation order after deafferentation supports hypotheses that gross limb rhythms and gross muscle activity patterns are controlled by a CPG and are robust to the loss of phasic limb sensory feedback. The loss of sensory feedback has been shown to result in an increase in the amplitude or RIA of activity in some muscles controlling limb movement in newts (Székely et al., 1969), cats (Grillner and Zangger, 1984) and the wings of locusts (Pearson and Wolf, 1987). In this study, the RIA of every muscle significantly increased after the loss of sensory feedback (Table S2). These interspecific differences in motor control variability after the loss of sensory feedback could be a result of differences in the sensory system among mammals, amphibians and fishes (Matthews, 1972; Prochazka et al., 2002; Romanovsky et al., 2007), the return of the CPG to its intrinsic default pattern, or both. In this study, we only transected the afferent nerves innervating the pectoral fin rays. Although any proximal proprioceptors associated with the pectoral fin would still be intact, the similarities in the resulting motor patterns after the complete loss of sensory feedback in tetrapod limbs and from only the fin rays of the pectoral fin in this study suggest that fin ray sensory feedback contributes significantly to the control of fin movement.

We suggest that increased muscle activity duration and the occurrence of overlapping activity between antagonistic muscles at both extremes of the fin stroke increase stability of the pectoral fin system after the loss of sensory feedback. The most common result of limb deafferentation across systems is an increase in the duration of muscle activity and overlap of activity between antagonistic muscles. The overlap of activity between antagonistic muscles after deafferentation is seen in the flight system of the locust (Pearson and Wolf, 1987), the limbs of newts (Székely et al., 1969) and the limbs of mammals (Grillner and Zangger, 1975; Perret and Cabelguen, 1976, 1980; Grillner and Zangger, 1984). Prolonged muscle activity and the presence of overlapping antagonistic muscle activity after deafferentation is also prominent in the pectoral fin of *S. quoyi* (Figs 6 and 7). In animals with intact sensory systems, the co-contraction of functionally antagonistic muscles commonly occurs during the completion of fine motor tasks, skilled movements and elaborate movements (Paillard, 1960). The co-contraction of antagonistic muscles is a significant feature of grading movements, joint fixation and general limb stability (Paillard, 1960; Székely et al., 1969). Limb stiffening by the co-contraction of antagonistic muscles also occurs in humans learning novel motor tasks (Bernstein, 1967; Milner and Cloutier, 1993). In the pectoral fin of *S. quoyi*, the co-contraction of antagonists likely results in increased joint stiffness and an increase the stability of fin movement.

Author contributions
Conceptualization: B.R.A., M.W.W., M.E.H.; Methodology: B.R.A., A.M.O., M.W.W., M.E.H.; Formal analysis: B.R.A., A.M.O., C.E.M.; Investigation: B.R.A., C.E.M.; Data curation: B.R.A., A.M.O., C.E.M.; Writing - original draft: B.R.A., M.W.W., M.E.H.; Writing - review & editing: B.R.A., A.M.O., M.W.W., M.E.H.; Visualization: B.R.A., A.M.O.; Supervision: M.W.W., M.E.H.; Project administration: M.E.H.; Funding acquisition: M.W.W., M.E.H.

References

Aiello, B. R., King, H. M. and Hale, M. E. (2014). Functional subdivision of fin protractor and retractor muscles underlies pelvic fin walking in the African lungfish *Protopterus annectens. J. Exp. Biol.* **217**, 3474-3482. doi:10.1242/jeb.105262

Aiello, B. R., Westneat, M. W. and Hale, M. E. (2017). Mechanosensation is evolutionarily tuned to locomotor mechanics. *Proc. Natl. Acad. Sci. USA* **114**, 4459-4464. doi:10.1073/pnas.1616839114

Aiello, B. R., Hardy, A. R., Westneat, M. W. and Hale, M. E. (2018). Fins as mechanosensors for movement and touch-related behaviors. *Integr. Comp. Biol.* **58**, 844-859. doi:10.1093/icb/icy065

Aiello, B. R., Olsen, A. M., Mathis, C. E., Westneat, M. and Hale, M. E. (2020). Data from: Pectoral fin kinematics and motor patterns are shaped by fin ray mechanosensation during steady swimming in *Scarus quoyi*. Dryad Dataset doi:10.5061/dryad.gtht76hhb

Alben, S., Madden, P. G. and Lauder, G. V. (2007). The mechanics of active fin-shape control in ray-finned fishes. *J. R Soc. Interface* **4**, 243-256. doi:10.1098/rsif.2006.0181

Barker, D. (1974). Muscle receptors. handbook of sensory physiology. *Springer-Verlag* **3**, 1-310. doi:10.1007/978-3-642-65945-4

Bernstein, N. A. (1967). Trends and problems in the study of investivation of physiology of activity. In *The Coordination and Regulation of Movements* (ed. N. A. Bernstein), pp. 441-466. Oxford: Pergamon.

Bosco, G. and Poppele, R. E. (2001). Proprioception from a spinocerebellar perspective. *Physiol. Rev.* **81**, 539-568. doi:10.1152/physrev.2001.81.2.539

Brown, T. G. and Sherrington, C. S. (1912). The rule of reflex response in the limb reflexes of the mammal and its exceptions. *J. Physiol.* **44**, 125-130. doi:10.1113/jphysiol.1912.sp001504

Cooper, B. Y., Glendinning, D. S. and Vierck, C. J. (1993). Finger movement deficits in the stumptail macaque following lesions of the fasciculus-cuneatus. *Somatosens. Mot. Res.* **10**, 17-29. doi:10.3109/08990229309028820

Daniel, T. L. and Combes, S. A. (2002). Flexible wings and fins: bending by inertial or fluid-dynamic forces? *Integr. Comp. Biol.* **42**, 1044-1049. doi:10.1093/icb/42.5.1044

Esposito, C. J., Tangorra, J. L., Flammang, B. E. and Lauder, G. V. (2012). A robotic fish caudal fin: effects of stiffness and motor program on locomotor performance. *J. Exp. Biol.* **215**, 56-67. doi:10.1242/jeb.062711

Fessard, A. and Sand, A. (1937). Stretch receptors in the muscles of fishes. *J. Exp. Biol.* **14**, 383-404.

Flammang, B. E. and Lauder, G. V. (2013). Pectoral fins aid in navigation of a complex environment by bluegill sunfish under sensory deprivation conditions. *J. Exp. Biol.* **216**, 3084-3089. doi:10.1242/jeb.080077

Flammang, B. E., Alben, S., Madden, P. G. A. and Lauder, G. V. (2013). Functional morphology of the fin rays of teleost fishes. *J. Morphol.* **274**, 1044-1059. doi:10.1002/jmor.20161

Fuchs, E., Holmes, P., David, I. and Ayali, A. (2012). Proprioceptive feedback reinforces centrally generated stepping patterns in the cockroach. *J. Exp. Biol.* **215**, 1884-1891. doi:10.1242/jeb.067488

Geerlink, P. J. and Videler, J. J. (1987). The relation between structure and bending properties of teleost fin rays. *Neth. J. Zool.* **37**, 59-80. doi:10.1163/002829687X00044

Grillner, S. (1975). Locomotion in vertebrates: central mechanisms and reflex interaction. *Physiol. Rev.* **55**, 247-304. doi:10.1152/physrev.1975.55.2.247

Grillner, S. (1985). Neurobiological bases of rhythmic motor acts in vertebrates. *Science* **228**, 143-148. doi:10.1126/science.3975635

Grillner, S. and Zangger, P. (1975). How detailed is the central pattern generation for locomotion? *Brain Res.* **88**, 367-371. doi:10.1016/0006-8993(75)90401-1

Grillner, S. and Zangger, P. (1979). On the central generation of locomotion in the low spinal cat. *Exp. Brain Res.* **34**, 241-261. doi:10.1007/BF00235671

Grillner, S. and Zangger, P. (1984). The effect of dorsal root transection on the efferent motor pattern in the cat's hindlimb during locomotion. *Acta Physiol. Scand.* **120**, 393-405. doi:10.1111/j.1748-1716.1984.tb07400.x

Hale, M. E., Day, R. D., Thorsen, D. H. and Westneat, M. W. (2006). Pectoral fin coordination and gait transitions in steadily swimming juvenile reef fishes. *J. Exp. Biol.* **209**, 3708-3718. doi:10.1242/jeb.02449

Hardy, A. R., Steinworth, B. M. Hale, M. E. (2016). Touch sensation by pectoral fins of the catfish *Pimelodus pictus. Proc. Roy. Soc. B* **283**. doi:10.1098/rspb.2015.2652

Higham, T. E., Malas, B., Jayne, B. C. and Lauder, G. V. (2005). Constraints on starting and stopping: behavior compensates for reduced pectoral fin area during braking of the bluegill sunfish Lepomis macrochirus. *J. Exp. Biol.* **208**, 4735-4746. doi:10.1242/jeb.01966

Hnik, P., Vejsada, R. and Kasicki, S. (1982). EMG changes in rat hind limb muscles following bilateral deafferentation. *Pflugers Arch.* **395**, 182-185. doi:10.1007/BF00584806

Hoyt, D. F. and Taylor, C. R. (1987). Gait and the energetics of locmotion in horses. *Nature* **292**, 239-240. doi:10.1038/292239a0

Kahn, J. C., Flammang, B. E. and Tangorra, J. L. (2012). Hover kinematics and distributed pressure sensing for force control of biorobotic fins. *Proceedings of the IEEE/RSJ International Conference on Intelligent Robots and Systems*, 1460-1466. doi:10.1109/IROS.2012.6386066

Katz, P. S. and Harris-Warrick, R. M. (1990). Neuromodulation of the crab pyloric central pattern generator by serotonergic/cholinergic proprioceptive afferents. *J. Neurosci.* **10**, 1495-1512. doi:10.1523/JNEUROSCI.10-05-01495.1990

Korsmeyer, K. E., Steffensen, J. F. and Herskin, J. (2002). Energetics of median and paired fin swimming, body and caudal fin swimming, and gait transition in parrotfish (Scarus schlegeli) and triggerfish (Rhinecanthus aculeatus). *J. Exp. Biol.* **205**, 1253-1263.

Lauder, G. V. and Drucker, E. G. (2004). Morphology and experimental hydrodynamics of fish fin control surfaces. *IEEE J. Ocean. Eng.* **29**, 556-571. doi:10.1109/JOE.2004.833219

Lauder, G. V., Madden, P. G. A., Tangorra, J. L., Anderson, E. and Baker, T. V. (2011). Bioinspiration from fish for smart material design and function. *Smart Mater. Struct.* **20**, 094014. doi:10.1088/0964-1726/20/9/094014

Loeb, G. E. and Gans, C. (1986). *Electromyography for Experimentalists*. Chicago: University of Chicago Press.

Lowenstein, O. (1956). Pressure receptors in the fins of the dogfish, Scyliorhinus canicula. *J. Exp. Biol.* **33**, 417-421.

Maeda, N., Miyoshi, S. and Toh, H. (1983). First observation of a muscle spindle in fish. *Nature* **302**, 61-62. doi:10.1038/302061a0

Margaria, R. (1938). Sulla fisiologica e specialmente sul consumo energetico della corsa a varie velocita ed inclinazioni del terreno: Atti Accad. Naz. Lincei Menorie. In *Biomechanics and Energetics of Muscular Exercise* (ed. H. T. Edwards), pp. 69-75. Oxford: Clarendon Press.

Matthews, P. B. (1972). *Mammalian Muscle Receptors and their Central Actions*. Baltimore, MD: The Williams and Wilkins Co.

Milner, T. E. and Cloutier, C. (1993). Compensation for mechanically unstable loading in voluntary wrist movement. *Exp. Brain Res.* **94**, 522-532. doi:10.1007/BF00230210

Nathan, P. W., Smith, M. C. and Cook, A. W. (1986). Sensory effects in man of lesions of the posterior columns and of some other afferent pathways. *Brain* **109**, 1003-1041. doi:10.1093/brain/109.5.1003

Olsen, A. M. (2017). Feeding ecology is the primary driver of beak shape diversification in waterfowl. *Funct. Ecol.* **31**, 1985-1995. doi:10.1111/1365-2435.12890

Olsen, A. M. and Westneat, M. W. (2015). StereoMorph: an R package for the collection of 3D landmarks and curves using a stereo camera set-up. *Methods Ecol. Evol.* **6**, 351-356. doi:10.1111/2041-210X.12326

Ono, R. D. (1979). Sensory nerve endings of highly mobile structures in two marine teleost fishes. *Zoomorphologie* **92**, 107-114. doi:10.1007/BF01001533

Ono, R. D. (1982). Proprioceptive endings in the myotomes of the pickerel (Teleostei, Esocidae). *J. Fish Biol.* **21**, 525-535. doi:10.1111/j.1095-8649.1982.tb02857.x

Paillard, J. (1960). The patterning of skilled movements, Sec. 1: Neurophysiology. In *Handbook of Physiology*, Vol. 3 (ed. J. Field, H. W. Magoun and V. E. Hall), pp. 1679-1708. Washington: Amer. Physiol. Ass.

Pansini, S. (1888). Delle terminazioni dei nervi sui tendini nei Vertebrati. *Boll. Soc. Nat. Napoli.* **1**, 135-160.

Pearson, K. G. and Wolf, H. (1987). Comparison of motor patterns in the intact and deafferented flight system of the locust. I. Electromyographic analysis. *J. Comp. Physiol. A.* **160**, 259-268. doi:10.1007/BF00609731

Perret, C. and Cabelguen, J.-M. (1976). Central and reflex participation in timing of locomotor activations of a bifunctional muscle, semi-tendinosus, in cat. *Brain Res.* **106**, 390-395. doi:10.1016/0006-8993(76)91035-0

Perret, C. and Cabelguen, J.-M. (1980). Main characteristics of the hindlimb locomotor cycle in the decorticate cat with special reference to bifunctional muscles. *Brain Res.* **187**, 333-352. doi:10.1016/0006-8993(80)90207-3

Polit, A. and Bizzi, E. (1978). Processes controlling arm movements in monkeys. *Science* **201**, 1235-1237. doi:10.1126/science.99813

Polit, A. and Bizzi, E. (1979). Characteristics of motor programs underlying arm movements in monkeys. *J. Neurophysiol.* **42**, 183-194. doi:10.1152/jn.1979.42.1.183

Prochazka, A., Gritsenko, V. and Yakovenko, S. (2002). Sensory control of locomotion: reflexes versus higher-level control. In *Sensorimotor Control* (ed. S. G. Gan-devia, U. Proske and D. G. Stuart), pp. 1-13. London, U.K: Kluwer Academic/Plenum Publishers.

Romanovsky, D., Moseley, A. E., Mrak, R. E., Taylor, M. D. and Dobretsov, M. (2007). Phylogenetic preservation of alpha3 Na+,K+-ATPase distribution in

vertebrate peripheral nervous systems. *J. Comp. Neurol.* **500**, 1106-1116. doi:10.1002/cne.21218

Ross, C. F., Blob, R. W., Carrier, D. R., Daley, M. A., Deban, S. M., Demes, B., Gripper, J. L., Iriarte-Diaz, J., Kilbourne, B. M., Landberg, T. et al. (2013). The evolution of locomotor rhythmicity in tetrapods. *Evolution* **67**, 1209-1217. doi:10.1111/evo.12015

Sainburg, R. L., Poizner, H. and Ghez, C. (1993). Loss of proprioception produces deficits in interjoint coordination. *J. Neurophysiol.* **70**, 2136-2147. doi:10.1152/jn.1993.70.5.2136

Sainburg, R. L., Ghilardi, M. F., Poizner, H. and Ghez, C. (1995). Control of limb dynamics in normal subjects and patients without proprioception. *J. Neurophysiol.* **73**, 820-835. doi:10.1152/jn.1995.73.2.820

Sanes, J. N., Mauritz, K. H., Dalakas, M. C. and Evarts, E. V. (1985). Motor control in humans with large-fiber sensory neuropathy. *Hum. Neurobiol.* **4**, 101-114.

Sherrington, C. S. (1913). Further observations on the production of reflex stepping by combination of reflex excitation with reflex inhibition. *J. Physiol.* **47**, 196-214. doi:10.1113/jphysiol.1913.sp001620

Sokal, R. R. and Braumann, C. A. (1980). Significance tests for coefficients of variation and variability profiles. *Systematic Biol.* **29**, 50-66. doi:10.1093/sysbio/29.1.50

Székely, G., Czeh, G. and Voros, G. (1969). The activity pattern of limb muscles in freely moving normal and deafferented newts. *Exp. Brain Res.* **9**, 53-72. doi:10.1007/BF00235451

Tangorra, J. L., Lauder, G. V., Hunter, I. W., Mittal, R., Madden, P. G. A. and Bozkurttas, M. (2010). The effect of fin ray flexural rigidity on the propulsive forces generated by a biorobotic fish pectoral fin. *J. Exp. Biol.* **213**, 4043-4054. doi:10.1242/jeb.048017

Thorsen, D. H. and Hale, M. E. (2007). Neural development of the zebrafish (Danio rerio) pectoral fin. *J. Comp. Neurol.* **504**, 168-184. doi:10.1002/cne.21425

Thoumie, P. and Do, M. C. (1996). Changes in motor activity and biomechanics during balance recovery following cutaneous and muscular deafferentation. *Exp. Brain Res.* **110**, 289-297. doi:10.1007/BF00228559

Vogel, S. and Labarbera, M. (1978). Simple flow tanks for research and teaching. *Bioscience* **28**, 638-643. doi:10.2307/1307394

Walker, J. A. and Westneat, M. W. (1997). Labriform propulsion in fishes: kinematics of flapping aquatic flight in the bird wrasse Gomphosus varius (Labridae). *J. Exp. Biol.* **200**, 1549-1569.

Walker, J. A. and Westneat, M. W. (2002a). Kinematics, dynamics, and energetics of rowing and flapping propulsion in fishes. *Integr. Comp. Biol.* **42**, 1032-1043. doi:10.1093/icb/42.5.1032

Walker, J. A. and Westneat, M. W. (2002b). Performance limits of labriform propulsion and correlates with fin shape and motion. *J. Exp. Biol.* **205**, 177-187.

Westneat, M. W. (1996). Functional morphology of aquatic flight in fishes: Kinematics, electromyography, and mechanical modeling of labriform locomotion. *Am. Zool.* **36**, 582-598. doi:10.1093/icb/36.6.582

Westneat, M. and Walker, J. (1997). Motor patterns of labriform locomotion: kinematic and electromyographic analysis of pectoral fin swimming in the labrid fish Gomphosus varius. *J. Exp. Biol.* **200**, 1881-1893.

Williams, R. and Hale, M. E. (2015). Fin ray sensation participates in the generation of normal fin movement in the hovering behavior of the bluegill sunfish (Lepomis macrochirus). *J. Exp. Biol.* **218**, 3435-3447. doi:10.1242/jeb.123638

Williams, R., Neubarth, N. and Hale, M. E. (2013). The function of fin rays as proprioceptive sensors in fish. *Nat. Commun.* **4**, 1729. doi:10.1038/ncomms2751

Wilson, D. M. and Gettrup, E. (1963). A stretch reflex controlling wingbeat frequency in grasshoppers. *J. Exp. Biol.* **40**, 171.

Wunderer, H. (1908). Über Terminalkörperchen der Anamnien. *Archiv für mikroskop. Anat. Entwicklungsmech.* **71**, 504-569. doi:10.1007/BF02979925

Yamamoto, I., Terada, Y., Nagamatu, T. and Imaizumi, Y. (1995). Propulsion system with flexible rigid oscillating fin. *IEEE J. Ocean. Eng.* **20**, 23-30. doi:10.1109/48.380249

Young, J., Walker, S. M., Bomphrey, R. J., Taylor, G. K. and Thomas, A. L. R. (2009). Details of insect wing design and deformation enhance aerodynamic function and flight efficiency. *Science* **325**, 1549-1552. doi:10.1126/science.1175928

Zhu, Q. and Shoele, K. (2008). Propulsion performance of a skeleton-strengthened fin. *J. Exp. Biol.* **211**, 2087-2100. doi:10.1242/jeb.016279